

# Characterization of Sn-Containing Polymer Chain Ends of Polybutadiene Using $^1\text{H}/^{13}\text{C}/^{119}\text{Sn}$ Triple-Resonance 3D-NMR

Weixia Liu, Takeshi Saito, Lan Li, and Peter L. Rinaldi\*

Department of Chemistry, Knight Chemical Laboratory, The University of Akron,  
190 E. Buchtel Commons, Akron, Ohio 44325-3601

Robert Hirst, Adel F. Halasa, and James Visintainer

Corporate Research, The Goodyear Tire & Rubber Company, 142 Goodyear Blvd., Akron, Ohio 44305

Received October 22, 1999; Revised Manuscript Received February 3, 2000

**ABSTRACT:**  $^1\text{H}/^{13}\text{C}/^{119}\text{Sn}$  triple-resonance 3D-NMR spectroscopy is used to characterize the tin-containing structures in the organotin polymer  $n\text{-Bu}_3\text{SnPBD}$  (PBD = polybutadiene). Triple-resonance techniques, when used together with pulsed field gradient coherence selection, permit selective detection of the structure fragments near  $^{119}\text{Sn}$  atom while removing intense signals of the PBD backbone from the spectrum. Three frequency dimensions provide enormous spectral dispersion, permitting the resolution of many signals that are not observable in 1D-NMR spectra. The simultaneous correlation of resonances from three nuclei provides a large amount of unambiguous atomic connectivity information. The capabilities of modern instruments are such that it is possible to perform these experiments without the benefit of isotopic labeling, despite the low concentration of chain ends and the low occurrence of fragments with  $^1\text{H}$ ,  $^{13}\text{C}$ , and  $^{119}\text{Sn}$  isotopes.

## Introduction

In the polymer industry, Sn-containing star-branched polymers have attracted considerable interest for their unique and valuable properties. For example, structures such as the ones described in this paper are thought to contribute to the improved performance characteristics of elastomers used in tires. Although  $^{119}\text{Sn}$  1D-NMR has been used to investigate the structures in the vicinity of the Sn branching site,<sup>1</sup> characterization of these materials is always a challenge due to severe resonance overlap and limited information present in 1D spectra, as well as the low receptivity of  $^{119}\text{Sn}$  and the low occurrence of Sn in the polymer structure. It is often difficult to assign the  $^{119}\text{Sn}$  NMR spectra on a firm basis, because of the limited information available in a 1D-NMR spectrum.

Recently,  $^1\text{H}/^{13}\text{C}/^{15}\text{N}$  triple-resonance, three-dimensional (3D)-NMR techniques have been powerful tools for biomolecular structure determination, where the molecules have been uniformly labeled with  $^{13}\text{C}$  and  $^{15}\text{N}$ .<sup>2</sup> Triple-resonance  $^1\text{H}/^{13}\text{C}/\text{X}$  3D-NMR methods have recently been used to study the microstructures of synthetic polymer, without the benefit of isotopic labeling. This early work was aided by the fact that the X nucleus was present on every monomer unit in the polymer chain and/or the presence of the NMR active isotopes of the X-nucleus in ca. 100% abundance (e.g.,  $^{19}\text{F}$  or  $^{31}\text{P}$ ). Here we show that  $^1\text{H}/^{13}\text{C}/^{119}\text{Sn}$  triple-resonance 3D-NMR can be used to obtain spectra of  $n\text{-Bu}_3\text{SnPBD}$  (PBD = polybutadiene) without resorting to isotopic labeling, despite the low natural abundance of both  $^{13}\text{C}$  and  $^{119}\text{Sn}$  (1.1% and 8.6%, respectively) and the presence of only one Sn-containing structure per polymer chain.  $^1\text{H}/^{13}\text{C}/^{29}\text{Si}$  3D-NMR where both  $^{13}\text{C}$  and  $^{29}\text{Si}$  are present in low natural abundance has been reported.<sup>5</sup> However, this represents the first report of

triple-resonance 3D-NMR for selective detection of a single site in a macromolecule without artificial enrichment of low abundance nuclei.

## Experimental Section

### Preparation of Star-Branched Organotin Polymers.

The premix of hexane/1,3-butadiene (80/20 w/w) was polymerized by adding  $n$ -butyllithium in hexane to prepare polybutadiene having ca. 5000 g mol<sup>-1</sup> molecular weight. All polymerizations were done under an inert atmosphere to ensure that the polybutadienyllithium chain ends were active. Then tri- $n$ -butyltin chloride was reacted with the polybutadiene-lithium living chain ends under an inert atmosphere to form the coupled polymer. The stoichiometry of the tin compound to the lithium living chain ends was in a molar ratio of Sn/Li = 1.0.

**General NMR.** NMR spectra were obtained using a Varian UNITYplus 750 MHz NMR spectrometer equipped with three broad radio-frequency channels, a Performa I pulsed field gradient accessory, and a Nalorac  $^1\text{H}/^{13}\text{C}/\text{X}/^2\text{H}$  (where X is tunable over the range of resonance frequencies from  $^{31}\text{P}$  to  $^{15}\text{N}$ ) four-channel probe equipped with a  $z$ -axis pulsed field gradient coil. Spectra were obtained from ca. 200 mg of the organotin polymer in 0.7 mL of  $\text{C}_6\text{D}_6$  unless otherwise mentioned. All NMR data were processed with Varian's VNMR software on a Sun workstation.  $\text{C}_6\text{D}_6$  was used as an internal reference for the  $^1\text{H}$  chemical shifts ( $\delta_{\text{H}} = 7.18$  for residual protons). TMS was used as an external reference for the  $^{13}\text{C}$  chemical shifts ( $\delta_{^{13}\text{C}} = 0$ ). Tetrabutyltin used as an external reference for the  $^{119}\text{Sn}$  chemical shifts ( $\delta_{^{119}\text{Sn}} = -11.5$ ).<sup>6</sup>

**Acquisition of 2D  $^1\text{H}-^{13}\text{C}$  and  $^1\text{H}-^{119}\text{Sn}$  HMQC NMR Spectra.** The  $^1\text{H}-^{13}\text{C}$  HMQC-NMR spectrum was obtained with the States method<sup>7</sup> of phase-sensitive detection, using 90° pulses for  $^1\text{H}$  and  $^{13}\text{C}$  of 10.7 and 36.0  $\mu\text{s}$ , respectively, a relaxation delay of 1.5 s, a delay  $\Delta$  of 1.79 ms (based on  $^1J_{\text{CH}} = 140$  Hz), and a 0.049 s acquisition time (with GARP1<sup>8</sup>-modulated  $^{13}\text{C}$  decoupling). Eight transients were averaged for each of 512 increments during  $t_1$ , and 576 points were collected during  $t_2$ . The evolution times were incremented to provide the equivalent of a 10 015 Hz spectral width in the  $f_1$  dimension, and a 5999 Hz spectral width was used in the  $f_2$  dimension. The strengths of the three 2.0 ms PFG's were  $g_1 = 0.100$ ,  $g_2 = 0.100$ , and  $g_3 = -0.0503$  T m<sup>-1</sup>.<sup>9</sup> The total

\* Corresponding author: telephone 330-972-5990; Fax 330-972-5256; E-mail PeterRinaldi@uakron.edu.

experiment time was ca. 2 h. The data were zero-filled to  $2048 \times 1024$  points and weighted with a shifted sinebell function before Fourier transformation.

The following parameters were used in the  $^1\text{H}$ - $^{119}\text{Sn}$  PFG-HMQC experiment:  $^1\text{H}$  and  $^{119}\text{Sn}$   $90^\circ$  pulse widths of 10.7 and 33.0  $\mu\text{s}$ , respectively; 5999 and 3622 Hz spectral widths in the  $^1\text{H}$  ( $f_2$ ) and  $^{119}\text{Sn}$  ( $f_1$ ) dimensions, respectively; a relaxation delay of 1.5 s, a delay  $\Delta = 3.79$  ms optimized for  $1/(4 \times {}^2J_{\text{Hsn}})$ , and a 0.048 s acquisition time with MPF7<sup>10</sup>-modulated  $^{119}\text{Sn}$  decoupling. Eight transients were averaged for each of 512 increments during  $t_1$ , and 576 points were sampled during  $t_2$ . The strengths of the three 2.0 ms PFG's were  $g_1 = 0.100$ ,  $g_2 = 0.100$ , and  $g_3 = -0.0748 \text{ T m}^{-1}$ . The data were processed with a shifted sinebell weighting function, and the spectrum was displayed in the magnitude-mode in both dimensions. 2D Fourier transformation was performed on a  $2048 \times 1024$  matrix.

**Acquisition of 3D  $^1\text{H}/^{13}\text{C}/^{119}\text{Sn}$  NMR Spectra.** The 3D  $^1\text{H}/^{13}\text{C}/^{119}\text{Sn}$  NMR spectra were collected with the States method of phase-sensitive detection in all three dimensions with  $90^\circ$  pulses for  $^1\text{H}$ ,  $^{13}\text{C}$ , and  $^{119}\text{Sn}$  of 10.7, 36.0, and 33.0  $\mu\text{s}$ , respectively, a relaxation delay of 1.5 s,  $\Delta = 1.79$  ms (based on  $^1J_{\text{CH}} = 140 \text{ Hz}$ ), and acquisition time 0.048 s (with simultaneous  $^{13}\text{C}$  MPF7 decoupling and  $^{119}\text{Sn}$  MPF7 decoupling). Eight transients were averaged for each of  $2 \times 64$  increments during  $t_1$ ,  $2 \times 24$  increments during  $t_2$ , and 576 points in  $t_3$ . Three separate experiments were performed, each with  $\tau = 0.81$ , 12.5, and 5.0 ms (based on  $^1J_{^{13}\text{C}^{119}\text{Sn}} = 310 \text{ Hz}$ ,  $^3J_{^{13}\text{C}^{119}\text{Sn}} = 20 \text{ Hz}$ , and  $^2,3J_{^{13}\text{C}^{119}\text{Sn}} = 50 \text{ Hz}$ ). The evolution times were incremented to provide the equivalent of a 11 001 Hz spectral width in the  $f_1$  dimension, a 3997 Hz spectral width in the  $f_2$  dimension, and a 5999 Hz spectral width in the  $f_3$  dimension. The durations and amplitudes of gradient pulses were 2.0, 1.0, and 1.0 ms and 0.2, 0.2, and 0.074 T/m, respectively. The first gradient pulse was used as a homospoil pulse whose strength is not critical compared with the others. The ratio of the second and the third gradient pulses was set on the basis of the ratio of the  $^1\text{H}$  and  $^{119}\text{Sn}$  resonance frequencies. The total experiment time was ca. 36 h. The data were zero-filled to a  $1024 \times 256 \times 256$  matrix and weighted with a Gaussian function before Fourier transformation. Digital signal processing was applied to reduce the  $f_1$  spectral width to 1999 Hz.

## Results and Discussion

The  $n\text{-Bu}_3\text{SnPBD}$  was prepared by anionic polymerization of 1,3-butadiene (BD) to obtain a living polymer having ca. 5000 molecular weight,<sup>11</sup> which was capped with the  $n\text{-Bu}_3\text{SnCl}$ . If only the monomer units directly bound to Sn are considered, there are three possible chain end structures 1–3, depending on the stereo- and regiochemistry of Sn addition to the terminal repeat unit.

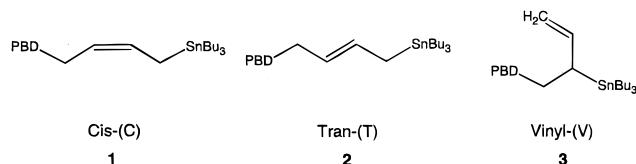
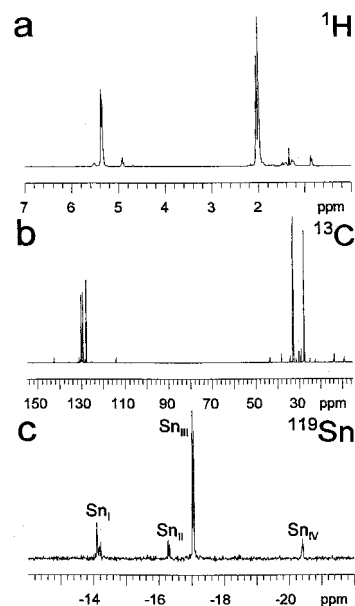
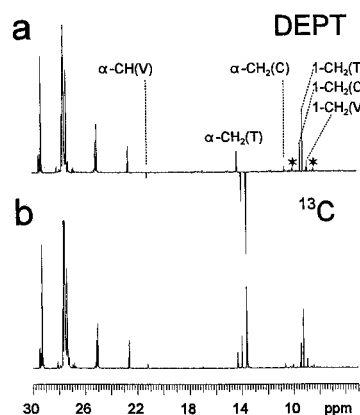


Figure 1 shows the aliphatic regions from the  $^1\text{H}$ ,  $^{13}\text{C}$ , and  $^{119}\text{Sn}$  1D-NMR spectra of  $n\text{-Bu}_3\text{SnPBD}$ . On the basis of the work of Senn et al.<sup>12</sup> and Werstler,<sup>13</sup> a ratio of *cis*-(C) and *trans*-1,4-butadiene (T) units to vinyl-1,2-butadiene (V) units of 9:1 is calculated from the  $^1\text{H}$  and  $^{13}\text{C}$  spectra. The 1D  $^{119}\text{Sn}$  spectrum shows four types of Sn species labeled I–IV in Figure 1c. Within each group of resonances there is additional fine structure from the different structures present in the second repeat unit from the chain end. Expansions from the aliphatic region of the DEPT<sup>14</sup> and  $^{13}\text{C}$  spectra are



**Figure 1.** 1D-NMR spectra of  $n\text{-Bu}_3\text{SnPBD}$  in  $\text{C}_6\text{D}_6$  collected at  $30^\circ\text{C}$ : (a) expansion of methylene region from 750 MHz  $^1\text{H}$  spectrum; (b) 188 MHz  $^{13}\text{C}$  spectrum with  $^1\text{H}$  decoupling; (c) 111.8 MHz  $^{119}\text{Sn}$  spectrum.



**Figure 2.** Expansions from the aliphatic regions of the 188.6 MHz 1D-NMR spectra: (a) DEPT-135 spectrum; (b) standard  $^{13}\text{C}$  NMR spectrum.

shown in Figure 2. Coupling constants ( $^1J_{^{13}\text{C}^{119}\text{Sn}} = 310 \text{ Hz}$ ) can be obtained from the peaks in the 8–11 ppm region of the  $^{13}\text{C}$  NMR in Figure 2, which exhibit the characteristic appearance of signals flanked by the components of the doublets from coupling between  $^{13}\text{C}/^{117}\text{Sn}$  (7.8% abundance) and  $^{13}\text{C}/^{119}\text{Sn}$  (8.6% abundance) satellites. It is still quite difficult to detect resonances from the BD repeat units attached to Sn atoms because their intensities are considerably weaker than the main-chain repeat unit signals.

The peaks in the DEPT-135 (distortionless enhancement by polarization transfer) spectrum, shown in Figure 2a, can be compared with corresponding region from the standard  $^{13}\text{C}$  spectrum shown in Figure 2b. Quaternary carbon atoms give no signals in the DEPT spectrum. The positive peaks in Figure 2a represent the  $\text{CH}_2$  groups in the structures, and negative peaks represent the  $\text{CH}$  and  $\text{CH}_3$  groups in the structures. The resonances labeled 1- $\text{CH}_2(\text{C})$ , 1- $\text{CH}_2(\text{T})$ , and 1- $\text{CH}_2(\text{V})$  are attributed to the  $\alpha$ -methylene carbons of the butyl groups. The resonances labeled  $\alpha\text{-CH}_2(\text{T})$  and  $\alpha\text{-CH}_2(\text{C})$  are attributed to the  $\alpha$ -methylene carbon of PBD (bound to tin) from *cis*/*trans*-1,4-butadiene units on the poly-

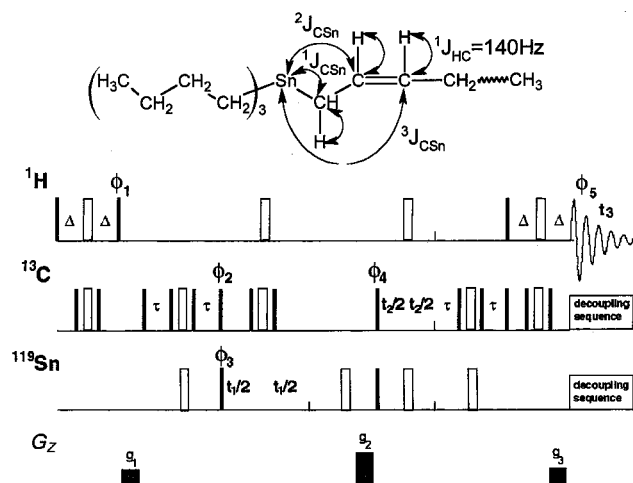


**Figure 3.** Diagram of the pulse sequence used for the  $^1\text{H}/^{13}\text{C}/^{119}\text{Sn}$  3D-NMR experiment:  $\phi_1 = \phi_2 = y$ ;  $\phi_3 = x, -x$ ;  $\phi_4 = y, y, -y, -y$ ;  $\phi_5 = x, -x, -x, x$ ; two spectra were collected with different sign of the first PFG and combined to obtain a pure absorption spectrum in  $f_2$ ,<sup>22</sup> and  $\phi_4$  was incremented according to the States method<sup>7</sup> during  $t_2$  to provide a hypercomplex phase-sensitive 3D data set. Additional PFG's were added to destroy undesired NMR signal components.

mer chain. The resonance labeled  $\alpha\text{-CH(V)}$  is attributed to the methine carbon bound to tin of vinyl units on the polymer chain. The satellites for  $^{13}\text{C}$  atoms bound to  $^{119}\text{Sn}$  and  $^{117}\text{Sn}$  are marked with asterisks flanking the signals near 9 ppm. From these peaks it is possible to determine  $^1J_{^{13}\text{C}^{119}\text{Sn}} = 313\text{ Hz}$  and  $^1J_{^{13}\text{C}^{117}\text{Sn}} = 299\text{ Hz}$ .

Figure 3 shows the pulse sequence used to collect the  $^1\text{H}/^{13}\text{C}/^{119}\text{Sn}$  3D-NMR shift correlation NMR spectra. This sequence is adapted from one of the first reported versions of the HNCA pulse sequence used to study proteins.<sup>15</sup> Use of this modified version of the pulse sequence can result in two improvements in signal-to-noise.<sup>16</sup> The experiment uses  $^1J_{\text{CH}}$  and  $^1J_{\text{CSn}}$  to sequentially transfer coherence along the path  $^1\text{H} \rightarrow ^{13}\text{C} \rightarrow ^{119}\text{Sn} \rightarrow ^{13}\text{C} \rightarrow ^1\text{H}$  as illustrated by the structure in Figure 3. Evolution times are inserted where the coherence resides on  $^{119}\text{Sn}$  and  $^{13}\text{C}$  as previously described, and the gradient area ratios,  $g_2/g_3 = \nu_{\text{H}}/\nu_{\text{Sn}}$ , are set to selectively refocus and detect signals originating from  $^1\text{H}/^{13}\text{C}/^{119}\text{Sn}$  spin systems [ $0.011$  (abundance of  $^{13}\text{C}$ )  $\times$   $0.086$  (abundance of  $^{119}\text{Sn}$ )  $\div$   $100$  (degree of polymerization) =  $0.09\%$  of the protons]. The experiment is made more difficult by the fact that there are many possible structures for the Sn-containing sites. If all these factors are considered, one recognizes that successful completion of an experiment requires detection of signals with relative intensity 1 from the chain end structures, while uniformly and completely suppressing the signals of intensity 1 000 000 from the remainder of the protons in the sample!

Figure 4a shows the  $^1\text{H}-^{13}\text{C}$  heteronuclear multiple quantum coherence (HMQC)<sup>17</sup> 2D-NMR spectrum of  $n\text{-Bu}_3\text{SnPBD}$ . The spectrum is dominated by the C-H correlations from the main-chain repeat units, which obscure many of the resonances from the Sn chain ends. Figure 4b shows a projection of the  $^1\text{H}/^{13}\text{C}/^{119}\text{Sn}$  3D-NMR spectrum of  $n\text{-Bu}_3\text{SnPBD}$  onto the  $f_1f_3$  plane. This plot shows only the correlations between the resonances of  $^1\text{H}$  and  $^{13}\text{C}$  atoms in  $\text{CH}_n$  groups bound to  $^{119}\text{Sn}$ . The remainder of the signals from nuclei that are not part of the  $^1\text{H}/^{13}\text{C}/^{119}\text{Sn}$  spin system are removed from the spectrum. Most of the peaks observed in the projection

of 3D-NMR spectrum are hidden in the HMQC spectrum by the methylene signals of the main-chain repeat units.

Figure 4c shows a plot of the  $^1\text{H}-^{119}\text{Sn}$  HMQC spectrum of  $n\text{-Bu}_3\text{SnPBD}$  obtained using  $\tau$  delays optimized for  $^2J_{\text{HSn}} = 66\text{ Hz}$ . Four major Sn species are detected, having  $^{119}\text{Sn}$  chemical shifts of  $-14.2$ ,  $-16.3$ ,  $-17.0$ , and  $-20.4\text{ ppm}$ , corresponding to the peaks seen in the  $^{119}\text{Sn}$  1D-NMR spectrum. At these  $^{119}\text{Sn}$  chemical shifts, peaks in the aliphatic region are observed in the  $f_2$  dimension at  $\delta^1_{\text{H}} = 0.9$  and  $1.7$ . It would be preferable to use the  $^1\text{H}-^{119}\text{Sn}$  HMQC technique to prove the structure if it were not for the fact that it is not possible to distinguish between structures having *cis*- and *trans*-1,4-butadiene units in **1** and **2** based on  $^1\text{H}$  chemical shift.

The HNCA sequence has been used primarily to identify direct H-N-C $_{\alpha}$  attachments using  $^1J_{\text{NH}}$  and  $^1J_{\text{CN}}$  couplings in amino acid fragments. The small magnitude of multiple-bond  $^{13}\text{C}-^{15}\text{N}$  couplings makes it difficult to detect  $^1\text{H}-^{15}\text{N}$  and  $^1\text{H}-^{13}\text{C}$  correlations when coupling is between atoms separated by more than one bond in large molecules.

Heteronuclear spin-spin coupling constants can be used to provide valuable information concerning the structure of molecules. The range of multiple-bond  $^{13}\text{C}-^{119}\text{Sn}$  coupling constants ( $^nJ_{^{13}\text{C}^{119}\text{Sn}}$ ) varies with the number and types of bonds between  $^{13}\text{C}$  and  $^{119}\text{Sn}$  atoms. Table 1 summarizes  $^nJ_{^{13}\text{C}^{119}\text{Sn}}$  coupling constants<sup>18,19</sup> for various aliphatic and olefinic organotin species. The range of two bond coupling constants ( $^2J_{^{13}\text{C}^{119}\text{Sn}}$ ) is  $20\text{--}50\text{ Hz}$ . Even three-bond couplings between  $^{13}\text{C}$  and  $^{119}\text{Sn}$  can be significant. In most cases, it is found that  $|^3J_{\text{C-Sn}}| > |^2J_{\text{C-Sn}}|$ .

This makes it possible to perform the 3D  $^1\text{H}-^{13}\text{C}-^{119}\text{Sn}$  experiment in one of three ways to obtain different structural information. If a spectrum is collected with  $\tau = 1/(4 \times ^1J_{^{13}\text{C}^{119}\text{Sn}}) = 0.81\text{ ms}$ , slices at each of the  $^{119}\text{Sn}$  shifts will only contain C-H chemical shift correlations for  $\text{CH}_n$  groups directly bound to  $^{119}\text{Sn}$ . If a spectrum is collected with  $\tau = 1/(4 \times ^nJ_{^{13}\text{C}^{119}\text{Sn}}) = 12.5\text{ ms}$ , then slices at each of these  $^{119}\text{Sn}$  shifts will contain C-H correlations predominantly from  $\text{CH}_n$  groups two bonds away from  $^{119}\text{Sn}$ . Likewise, if a spectrum is collected with  $\tau = 1/(4 \times ^nJ_{^{13}\text{C}^{119}\text{Sn}}) = 5.0\text{ ms}$ , then slices at each of the  $^{119}\text{Sn}$  shifts will contain C-H correlations predominantly from  $\text{CH}_n$  groups three bonds away from  $^{119}\text{Sn}$ . Although one might envision continuing the series to identify  $\text{CH}_n$  groups four and five bonds away from Sn, typically  $^nJ_{\text{C-Sn}} < 5\text{ Hz}$  for  $n > 3$ . Broad lines, from efficient  $T_2$  relaxation in these polymers, hinder attempts to use coherence transfer based on the small couplings in these systems. Combined data from the three experiments provide information about Sn-C-H, Sn-C-C-H, and Sn-C-C-C-H fragments, to identify the bonding pattern in the molecule, and resolve all the resonances of  $^1\text{H}$ ,  $^{13}\text{C}$ , and  $^{119}\text{Sn}$ .

3D spectra obtained with  $\tau$  delays optimized for two- and three-bond  $^{13}\text{C}-^{119}\text{Sn}$  couplings will also contain weak cross-peaks from one-bond couplings. There are methods, using  $J$ -filtering, to remove these cross-peaks; however, these would require a more complicated and longer pulse sequence, permitting more time for signal attenuation (from relaxation). However, simplification through  $J$ -filtering is unnecessary because the 3D-NMR spectra are simple, the cross-peaks are simple and well-dispersed, and the cross-peaks from one-bond correla-

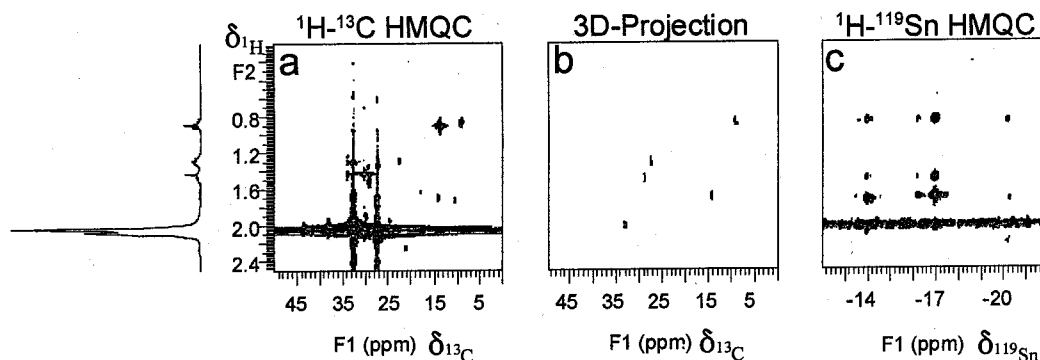


**Figure 4.**  $^1\text{H}/^{13}\text{C}/^{119}\text{Sn}$  2D- and 3D-NMR spectra of  $n\text{-Bu}_3\text{SnPBD}$  (200 mg) in  $\text{C}_6\text{D}_6$ : (a)  $^1\text{H}-^{13}\text{C}$  HMQC 2D-NMR spectrum; (b) shows a projection of  $^1\text{H}/^{13}\text{C}/^{119}\text{Sn}$  3D-NMR spectrum onto the  $f_1f_3$  plane; (c)  $^1\text{H}-^{119}\text{Sn}$  HMQC 2D-NMR spectrum.

**Table 1.**  $^nJ_{^{13}\text{C}-^{119}\text{Sn}}$  Coupling Constants in the Organotin Compounds

compounds	$^nJ_{^{13}\text{C}-^{119}\text{Sn}}$ (Hz)		
	$n = 1$	$n = 2$	$n = 3$
$\text{Sn}(\text{CH}_2\text{CH}=\text{CH}_2)_4$	264.9	48.3	51.3
$\text{Sn}(\text{CH}_2\text{CH}_3)_4$	307.0	23.5	
$\text{Sn}(\text{CH}_2\text{CH}_2\text{CH}_3)_4$	313.4	20.1	51.4
$\text{Sn}(\text{CH}_2\text{CH}_2\text{CH}_2\text{CH}_3)_4$	313.7	19.3	52.0
$(\text{Me})_3\text{SnCHCH}_2\text{CH}_2$	502.8 (CH)	18.8	
	341.6 ( $\text{CH}_3$ )		
$(\text{Me})_3\text{SnCHCH}_2\text{CH}_2\text{CH}_2$	389.7 (CH)	23.3	57.6
	313.5 ( $\text{CH}_3$ )		
$(\text{Me})_3\text{SnCHCH}_2\text{CH}_2\text{CH}_2\text{CH}_2\text{CH}_2$	407.4 (CH)	14.4	57.5
	303.9 ( $\text{CH}_3$ )		

tions in the multiple-bond spectra can be readily identified by comparison with the spectrum obtained with  $\tau = 1/(4 \times {}^1J_{^{13}\text{C}-^{119}\text{Sn}})$ .

Figure 5 shows selected slices from three separate  $^1\text{H}/^{13}\text{C}/^{119}\text{Sn}$  3D-NMR spectra obtained from the experiments using  $\tau$  delays of 0.81, 12.5, and 5.0 ms, respectively. The slices shown in these figures are arranged in rows based on four different  $^{119}\text{Sn}$  chemical shifts  $\delta_{^{119}\text{Sn}} = -14.2, -16.3, -17.0$ , and  $-20.4$  ppm of the four possible chain end structures and are arranged in columns based on the  $\tau$  delays used to acquire the spectra. Each slice shows  $\delta_{^1\text{H}}$  vs  $\delta_{^{13}\text{C}}$  ( $f_1f_3$ ) correlations of  $\text{CH}_n$  groups bound to the  $^{119}\text{Sn}$  atom having a chemical shift corresponding to the position of that slice in the  $f_2$  dimension. Because long-range  $^{13}\text{C}-^{119}\text{Sn}$  couplings are large ( ${}^2J_{^{13}\text{C}-^{119}\text{Sn}}$  and  ${}^3J_{^{13}\text{C}-^{119}\text{Sn}}$  are expected to be in the range 20–50 Hz), it is possible to use these interactions to get long-range structural connectivities, even for these polymers where relaxation times are relatively short.

The slices in the first column, Figure 5a,d,g,j, are taken from a 3D-NMR spectrum with delays optimized for the large  ${}^1J_{^{13}\text{C}-^{119}\text{Sn}} = 310$  Hz; they show  $\delta_{^1\text{H}}$  and  $\delta_{^{13}\text{C}}$  correlations of  $\text{CH}_n$  groups directly bound to the  $^{119}\text{Sn}$  atom having a chemical shift that corresponds to the position of that slice in the  $f_2$  ( $\delta_{^{119}\text{Sn}}$ ) dimension. The correlations of  $\text{CH}_2$  groups labeled with 1 shown in Figure 5a,d,g,j are attributed to the butyl methylene group directly bound to the  $^{119}\text{Sn}$  atoms. The butyl-methylene correlations have nearly identical  $^1\text{H}$  and  $^{13}\text{C}$  chemical shifts in all slices. The correlations of  $\text{CH}_n$  groups labeled with  $\alpha$  shown in Figure 5a,d,g are attributed to the methylene carbon of the polymer chain, which is directly bound to the  $^{119}\text{Sn}$  atom. These cross-peaks are from polymer structures in which the first monomer is a *cis*- or *trans*-1,4-butadiene unit. In Figure 5a the  $\text{CH}_2$  resonance at  $\delta_{^{13}\text{C}} = 9.6$  (labeled  $\alpha$ ) is attributed to the first methylene carbon in a *cis*-1,4-

butadiene unit (C) on the polymer chain. In Figure 5d,g the  $\text{CH}_2$  resonances at  $\delta_{^{13}\text{C}} = 9.4$  are attributed to the first methylene carbon in the *trans*-1,4-butadiene unit (T) on the polymer chain.<sup>20</sup> The differences between the resonances in Figure 5d,g are most likely from the different structures present in the second monomer repeat unit from the chain end. The correlation labeled with  $\alpha$  ( $\delta_{^1\text{H}} = 2.2$ ,  $\delta_{^{13}\text{C}} = 21.3$ ) shown in Figures 5j is from the  $\text{CH}_n$  groups directly bound to the  $^{119}\text{Sn}$  atom whose chemical shift occurs at  $-20.4$  ppm. This is attributed to a methine group, based on the sign of the peak at 21.3 ppm in the DEPT-135 spectrum (Figure 2a). Consequently, the slice from the one-bond 3D-NMR in Figure 5j must be from the shift of a  $^{119}\text{Sn}$  bound to a polymer chain in which the first monomer unit is from a vinyl-1,2-butadiene unit (V).

The slices in the second column, Figure 5b,e,h,k, are taken from a 3D-NMR spectrum collected using delays optimized for  ${}^{2,3}J_{^{13}\text{C}-^{119}\text{Sn}} = 20$  Hz. They show the  $\delta_{^1\text{H}}$  vs  $\delta_{^{13}\text{C}}$  correlations of aliphatic  $\text{CH}_n$  groups two and three bonds from the  $^{119}\text{Sn}$  atom having a chemical shift corresponding to the position of those slices. The  $\text{CH}_n$  groups correlations labeled with 2 and 3, shown in Figure 5b,e,h,k, are attributed to the butyl group methylene carbons two and three bonds away from the  $^{119}\text{Sn}$  atom. The  $\text{CH}_n$  group correlation labeled with  $\beta$  shown in Figure 5k is attributed to the PBD  $\text{CH}_2$  group two bonds away from the  $^{119}\text{Sn}$  atom whose chemical shift occurs at  $-20.4$  ppm. This group is adjacent to a vinyl-1,2-butadiene unit.

The resonances of  $\text{CH}_2$  groups in the spectrum collected using delays optimized for  ${}^nJ_{^{13}\text{C}-^{119}\text{Sn}} = 20$  Hz are mainly from two bond correlations in the aliphatic regions. However, these slices also contain correlations from  $\text{CH}_n$  groups directly bound to the  $^{119}\text{Sn}$  atom. The latter correlations can easily be identified by comparison with the spectra in the first column ( ${}^1J_{^{13}\text{C}-^{119}\text{Sn}} = 310$  Hz). Cross-peaks in the slices are labeled with resonance assignments corresponding to the numbering in the structures above each column of slices. Two-bond couplings between  $^{119}\text{Sn}$  and olefinic carbons are near 50 Hz and so are observed in these slices.

The slices in the third column of Figure 5c,f,i,l are taken from a 3D-NMR spectrum collected with delays optimized for  ${}^{2,3}J_{^{13}\text{C}-^{119}\text{Sn}} = 50$  Hz. Two- and three-bond coupling between  $^{119}\text{Sn}$  and olefinic carbons are near 50 Hz. The key information regarding the structures is found by examining the slices having C–H correlation in the olefinic regions (Figure 5c,f,i). These slices contain correlations from olefinic CH groups at  $\delta_{^{13}\text{C}} = 123\text{--}130$ . Figure 5l contains correlations  $\beta'$  and  $\gamma'$ , characteristic of resonances from terminal vinyl (V) units at  $\delta_{^{13}\text{C}} =$

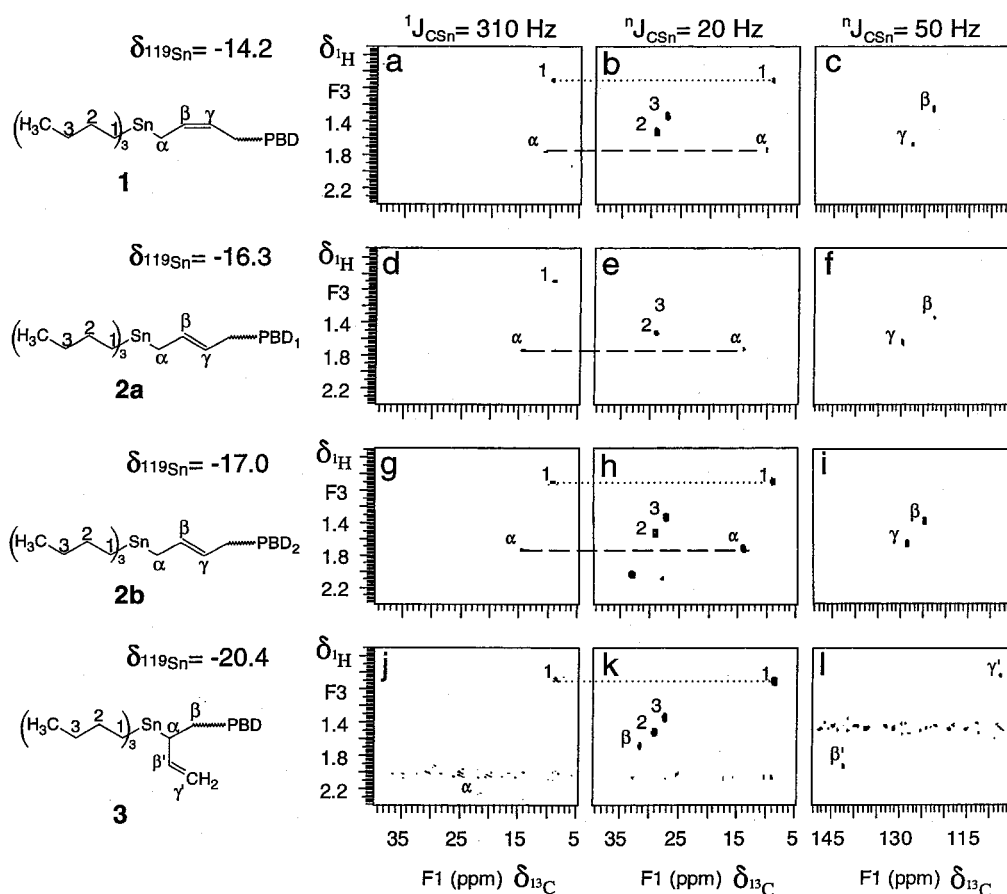


**Figure 5.** Slices from the  $^1\text{H}/^{13}\text{C}/^{119}\text{Sn}$  3D-NMR spectra of  $n\text{-Bu}_3\text{Sn}$  PBD in  $\text{C}_6\text{D}_6$ : (a–c), (d–f), (g–i), and (j–l) are slices corresponding to  $\delta_{^{119}\text{Sn}} = -14.2$ ,  $\delta_{^{119}\text{Sn}} = -16.3$ ,  $\delta_{^{119}\text{Sn}} = -17.0$ , and  $\delta_{^{119}\text{Sn}} = -20.4$ , respectively; (a, d, g, j) were obtained from the spectrum with  $\tau = 0.81$  ms (based on  $^1J_{^{13}\text{C}/^{119}\text{Sn}} = 310$  Hz), (b, e, h, k) were obtained from the spectrum with  $\tau = 12.5$  ms (based on  $^nJ_{^{13}\text{C}/^{119}\text{Sn}} = 20$  Hz) and show  $\delta_{^1\text{H}}$  and  $\delta_{^{13}\text{C}}$  correlation of aliphatic  $\text{CH}_n$  groups two bonds from  $^{119}\text{Sn}$ ; and (c, f, i, l) were obtained from the spectrum with  $\tau = 5.0$  ms (based on  $^nJ_{^{13}\text{C}/^{119}\text{Sn}} = 50$  Hz) and show  $\delta_{^1\text{H}}$  and  $\delta_{^{13}\text{C}}$  correlation of olefinic  $\text{CH}_n$  groups two and three bonds from  $^{119}\text{Sn}$ .

**Table 2. Chemical Shift Assignments of Star-Branched Polymer (ppm)**

position relative to Sn		$\delta_{\text{Sn}}$	$\alpha$		$\beta$		$\gamma$	
structure	branch		$\delta_{\text{H}}$	$\delta_{\text{C}}$	$\delta_{\text{H}}$	$\delta_{\text{C}}$	$\delta_{\text{H}}$	$\delta_{\text{C}}$
<b>1</b>	$-\text{CH}_2\text{CH}_2\text{CH}_2\text{CH}_3$	-14.2	0.87	9.6	1.49	29.4	1.29	27.5
	$\text{cis-CH}_2\text{CH=CHPBD}$		1.73	10.8	5.12	124.1	5.59	128.5
<b>2a</b>	$-\text{CH}_2\text{CH}_2\text{CH}_2\text{CH}_3$	-16.3	0.87	9.4	1.49	29.4	1.29	27.5
	$\text{trans-CH}_2\text{CH=CHPBD}_1$		1.70	14.5	5.21	123.7	5.54	130.7
<b>2b</b>	$-\text{CH}_2\text{CH}_2\text{CH}_2\text{CH}_3$	-17.0	0.87	9.4	1.49	29.4	1.29	27.5
	$\text{trans-CH}_2\text{CH=CHPBD}_2$		1.70	14.4	5.27	125.5	5.57	129.4
<b>3</b>	$-\text{CH}_2\text{CH}_2\text{CH}_2\text{CH}_3$	-20.4	0.87	9.1	1.49	29.4	1.29	27.5
	$\text{vinyl-CHCH}_2\text{PBD}$		2.23	21.3	1.65	30.3		
	$-\text{CH=CH}_2$				5.84	142.9	4.68	108.1

142.9 and 108.2 which are two and three bonds away from the Sn atom.

By combining the data from 1D-, 2D-, and 3D-NMR experiments, we can resolve all the  $^1\text{H}$ ,  $^{13}\text{C}$ , and  $^{119}\text{Sn}$  chemical shifts of the four structures **1**, **2a**, **2b**, and **3** unambiguously. These chemical shift assignments are summarized in Table 2. With the chemical shift assignments obtained from the 3D-NMR spectrum, it is possible to quantify the amount of each structure and compare these with the distribution of similar structures in the rest of the polymer chain.

After atomic connectivity patterns were identified by triple-resonance  $^1\text{H}/^{13}\text{C}/^{119}\text{Sn}$  3D-NMR, chain end monomer unit distribution can be conveniently extracted from  $^{13}\text{C}$  NMR spectra. Quantitative analysis was performed using a gated decoupling experiment and a relaxation delay of 15 s to suppress the nuclear Overhauser effect.

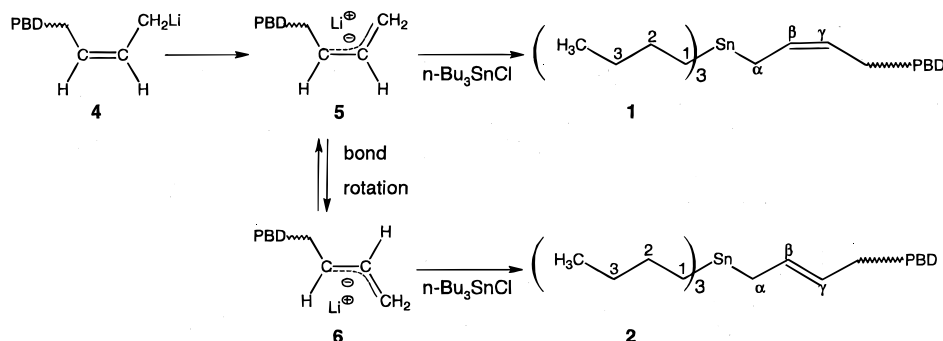
**Table 3. Quantitative Analysis of Organotin Polymer**

location	% of each monomer unit		
	<i>trans</i> -1,4-butadiene	<i>cis</i> -1,4-butadiene	vinyl-1,2-butadiene
main chain units	52	38	10
chain end first monomer units	69	20	11

Results from integration of the 1- $\text{CH}_2$ (T,C,V) signals in the  $^{13}\text{C}$  NMR spectrum at 188.6 MHz (Figure 2b) are summarized in Table 3.

It was found that the number of vinyl-1,2-butadiene (V) units at the chain ends is essentially the same as the percentage of these units in the main chain. The percentage of *trans*-1,4-butadiene (T) units increases at the chain end relative to the percentage of these units in the main chain.

Scheme 1



There are two steps to the preparation of polymer: (1) the PBD was prepared by anionic polymerization of 1,3-butadiene (BD) to obtain a living polymer; (2) this polymer was capped with the  $n\text{-Bu}_3\text{SnCl}$ . Scheme 1 shows a mechanism involving isomerization and termination reactions. Gerbert et al.<sup>21</sup> suggested a polymerization mechanism to explain the relative distribution of isomers at the chain end compared to the main chain. Initially, addition of a butadiene unit to the living chain end (4) forms a *cis*-allyl anion (5) which can isomerize to the *trans* anion (6). Both of these structures can add a 1,4-butadiene unit during propagation, based on the relative importance of kinetic and thermodynamic factors under the polymerization reaction conditions. When the capping reaction occurs, two factors should contribute to a lower fraction of C structures. The capping is done after some reaction time to permit bond rotation to the thermodynamically favorable *trans* isomer 6. Furthermore, the reaction of bulky  $n\text{-Bu}_3\text{SnCl}$  with 6 is much more favorable than its reaction with *cis* isomer 5. Sterics should be less important in the reaction of 1,4-butadiene with 5 and 6 during the polymer propagation reaction.

## Conclusions

Triple-resonance  $^1\text{H}/^{13}\text{C}/^{119}\text{Sn}$  3D-NMR methods can be enormously useful for characterizing the structures of organotin compounds. Application of such techniques are practicable, even when isotopic labeling is not possible, despite the extremely low concentration of species and low natural abundance of  $^{13}\text{C}$  and  $^{119}\text{Sn}$  studied in these polymer structures.

Triple-resonance combined with PFG techniques make it possible to detect signals from low occurrence structures such as those at the chain ends or the junctions in star-branched polymeric materials and more generally to study the structure of organometallic complexes.

Three-dimensional chemical shift correlation experiments provide enormous spectral dispersion and the unique correlation of three coupled nuclei provided polymer chain end structure information when coherence from the right combination of nuclei is chosen. It is possible to obtain resolved  $^1\text{H}$  and  $^{13}\text{C}$  correlation information based on the well-resolved  $^{119}\text{Sn}$  chemical shifts of resonances from the different structures in the organotin polymer chain ends. This is especially important in polymerization mechanism studies for the rubber industry. Similar applications of these experiments can be extremely useful in organometallic chemistry when the compounds contain a third NMR-active nucleus exhibiting resolvable  $J$ -coupling to  $^{13}\text{C}$ .

**Acknowledgment.** We acknowledge the National Science Foundation (DMR-9617477) and The Goodyear

Tire & Rubber Company for support of this research and the Kresge Foundation and donors to the Kresge Challenge program at The University of Akron for funds used to purchase the 750 MHz NMR instrument used in this work.

## References and Notes

- Hergenrother, W. L.; Doshak, J. M.; Brumbaugh, D. R.; Bethea, T. W.; Oziomek, J. *J. Polym. Sci.* **1995**, *33*, 143.
- (a) Bax, A.; Grzesiek, S. *Acc. Chem. Res.* **1993**, *26*, 131. (b) Cavanagh, J.; Fairbrother, W.; Palmer III, A. G.; Skelton, N. *Protein NMR Spectroscopy Principles and Practice*; Academic Press: San Diego, CA, 1996; Chapter 8.
- (a) Li, L.; Ray III, D. G.; Rinaldi, P. L.; Wang, H.-T.; Harwood, H. J. *Macromolecules* **1996**, *29*, 4706. (b) Li, L.; Rinaldi, P. L. *Macromolecules* **1996**, *29*, 4808.
- (a) Berger, S.; Bast, P. *Magn. Reson. Chem.* **1993**, *31*, 1021. (b) Saito, T.; Rinaldi, P. L. *J. Magn. Reson.* **1996**, *118*, 136. (c) Saito, T.; Rinaldi, P. L. *J. Magn. Reson.* **1998**, *130*, 135.
- Chai, M.; Pi, Z.; Tessier, C.; Rinaldi, P. L. *J. Am. Chem. Soc.* **1999**, *121*, 273.
- Wrackmeyer, B. *Annu. Rep. NMR Spectrosc.* **1985**, *16*, 73.
- States, D. J.; Haberkorn, R. A.; Ruben, D. J. *J. Magn. Reson.* **1982**, *48*, 286.
- Shaka, A. J.; Barker, P. B.; Freeman, R. *J. Magn. Reson.* **1985**, *64*, 547.
- (a) Rinaldi, P. L.; Keifer, P. A. *J. Magn. Reson.* **1994**, *108*, 259. (b) Vuister, G. W.; Boelens, R.; Kaptein, R.; Hurd, R. E.; John, B.; Van Zijl, P. C. M. *J. Am. Chem. Soc.* **1991**, *113*, 9688.
- (a) Fujiwara, T.; Nagayama, K. *J. Magn. Reson.* **1991**, *93*, 563. (b) Fujiwara, T.; Anai, T.; Kurihara, N.; Nagayama, K. *J. Magn. Reson.* **1993**, *104*, 103.
- Chang, C. C.; Halasa, A. F.; Miller, J. W. *J. Appl. Polym. Sci.* **1993**, *47*, 1589.
- Senn, W. L. *Anal. Chim. Acta* **1963**, *29*, 505.
- Werstler, D. D. *Rubber Chem. Technol.* **1980**, *53*, 1191.
- Pegg, D. T.; Doddrell, D. M.; Bendall, M. R. *J. Chem. Phys.* **1982**, *77*, 2745.
- (a) Ikura, M.; Kay, L. E.; Bax, A. *Biochemistry* **1990**, *29*, 4659. (b) Kay, L. E.; Ikura, M.; Tschudin, R.; Bax, A. *J. Magn. Reson.* **1990**, *89*, 496. (c) Clore, G. M.; Bax, A.; Driscoll, P. C.; Wingfield, P. T.; Gronenborn, A. M. *Biochemistry* **1990**, *29*, 8172.
- Farmer, B. T.; Venters, R. A.; Spicer, L. D.; Wittekind, M. G.; Muller, L. *J. Biomol. NMR* **1992**, *2*, 195.
- (a) Muller, L. *J. Am. Chem. Soc.* **1979**, *101*, 4481. (b) Bax, A.; Griffey, R. H.; Hawkins, B. L. *J. Magn. Reson.* **1983**, *55*, 301.
- (a) Omae, I. In *J. Organometallic Chemistry Library*, *21. Organotin Chemistry*; Elsevier Science Publishers: Amsterdam, 1989; p 294. (b) Mann, B. E. In *NMR and the Periodic Table*; Harris, R. K., Mann, B. E., Eds.; Academic Press: New York, 1978; p 361.
- Berger, S.; Mitchell, T. N. *Organometallics* **1992**, *11*, 3481.
- The downfield  $^{13}\text{C}$  resonance is assigned to the *trans* isomer on the basis of the fact that this isomer generally produces a downfield methylene resonance relative to the *cis* isomer in the polymer backbone (see ref 13).
- Gebert, W.; Hinz, J.; Sinn, H. *Makromol. Chem.* **1971**, *144*, 97.
- Keeler, J.; Neuhaus, D. *J. Magn. Reson.* **1985**, *63*, 454.

MA991771U